International Journal of Mathematical, Engineering and Management Sciences
Vol. 3, No. 4, 450–471, 2018
https://dx.doi.org/10.33889/IJMEMS.2018.3.4-033

Theoretical Study of Heat Transfer on Peristaltic Transport of Non-Newtonian Fluid Flowing in a Channel: Rabinowitsch Fluid Model

U. P. Singh
Department of Applied Sciences and Humanities
Rajkiya Engineering College, Sonbhadra, India

Amit Medhavi
Department of Mechanical Engineering
Kamla Nehru Institute of Technology, Sultanpur, India

R. S. Gupta
Coordinator Faculty of Engineering
University of Lucknow, India

Siddharth Shankar Bhatt
Department of Applied Sciences and Humanities
Kamla Nehru Institute of Technology, Sultanpur, India
Corresponding author: shankarbhatt56@gmail.com

(Received January 14, 2018; Accepted April 7, 2018)

Abstract
The present investigation is concerned with the problem of heat transfer and peristaltic flow of non-Newtonian fluid using Rabinowitsch fluid model through a channel under long wavelength and low Reynolds number approximation. Expressions for velocity, pressure gradient, pressure rise, friction force and temperature have been obtained. The effect of different parameters on velocity, pressure gradient, pressure rise, streamlines, friction force and temperature have been discussed through graphs.

Keywords- Peristalsis, Uniform channel, Heat transfer, Rabinowitsch fluid model.

1. Introduction

Peristalsis is an innate property of several biological systems and it occurs in the movement of urine from the kidney to bladder, vasomotion of small blood vessels, ovum transport in the fallopian tube and movement of chyme in the gastro-intestinal tract. It is an important transport mechanism not only in physiological processes but has a wide range of applications in engineering and industry. The principle of peristalsis has been used to develop pumps having physiological and industrial applications.

Probably the first pioneering investigation was done by Latham (1966) in which a theoretical attempt has been made to understand the peristaltic action. Fung and Yih, (1968), Shapiro et al. (1969), Yin and Fung (1969), Gupta and Seshadri (1976) and Machireddy and Kattamreddy (2016) have made a significant contribution to understand the peristaltic flow of Newtonian fluid. Theory of non-Newtonian fluid has attracted researchers during past few decades. To understand the flow properties of physiological fluids, Raju and Devanathan (1972) considered a non-Newtonian model (Power law fluid) of peristaltic motion in an axisymmetric tube caused due to the proliferation of sinusoidal wave on the walls. Considering the arbitrary wave shape, Kaimal

International Journal of Mathematical, Engineering and Management Sciences
Vol. 3, No. 4, 450–471, 2018
https://dx.doi.org/10.33889/IJMEMS.2018.3.4-033

(1978) studied the peristaltic motion of a particle-fluid mixture in an axisymmetrical tube at low Reynolds number. Misra and Pandey (2002) studied the peristaltic transport of blood in small blood vessels. In this study, the core layer is casson fluid and the outer layer is an incompressible Newtonian viscous fluid. Vajravelu et al. (2005) presented peristaltic pumping of incompressible fluid with Herschel-Bulkley fluid model in a channel. The analytical solution for velocity, pressure gradient and stream function were determined. Pandey and Chaube (2011) investigated wall properties during the action of peristaltic motion of couple stress fluid and disclosed the result that means velocity reduces by raising couple stress parameter and increases with increasing wall tension. Reddy et al. (2011) investigated the peristaltic motion of Carreau fluids through an inclined channel in presence of magnetic field. The perturbation method is used to analyze the flow. Akbar and Butt (2015) studied heat transfer under the action of the peristaltic flow of viscous fluid with Herschel-Bulkley fluid model while considering that fluid flowing through a non-uniform inclined channel. Study of peristaltic flow of non-Newtonian fluid with power law fluid model through the channel of varying width was done by Chaube et al. (2015). Consequences of changes in fluid behavior index, slip parameter and angle between the walls on velocity profile, pressure gradient and trapping phenomenon were discussed.

The study of heat transfer in association with peristalsis is essential because it plays a significant role in physiology. For instance, the thermodynamic features of blood are very useful in oxygenation and hemodialysis. Radhakrishnamacharya and Murty (1993) studied the heat transfer in the connection to peristaltic transport in a channel of varying width and found a perturbed solution for temperature and heat transfer coefficient. The problem of peristaltic pumping and heat transfer through an asymmetric channel was considered by Srinivas and Kothandapani (2008). Sinha et al. (2015) studied heat transfer analysis MHD flow through the asymmetric channel with variable viscosity. Bhatt et al. (2017) recently studied peristaltic transport and heat transfer through non-uniform geometry. Walls are assumed to be permeable and found that temperature decreases with increase in Darcy number. The study of heat and mass transfer in connection to the peristaltic transport of hyperbolic tangent fluid through a channel of varying width in presence of magnetic field was done by Sarvana et al. (2016).

Rabinowitsch fluid model is a well-established model for studying the non-Newtonian nature of the fluid. The shearing stress and shearing strain for the Rabinowitsch fluid model is connected by the relation as given below:

$$\tau_{YX} + \gamma \tau_{XY}^3 = \mu \frac{\partial U}{\partial Y} \tag{1}$$

where the nonlinear term γ is called coefficient of pseudoplasticity and the non-Newtonian nature of fluid depends on this parameter, μ is the viscosity of the fluid, U is velocity, X and Y are axial and transverse coordinate respectively. This model exhibits dilatant, Newtonian and pseudoplastic fluids nature for $\gamma < 0$, $\gamma = 0$ and $\gamma > 0$. Wada and Hayashi (1971) experimentally analyzed this model to justify theoretical results. Singh et al. (2011, 2012) and Singh, (2013) have utilized Rabinowitsch fluid model to investigate the performance of different types of hydrostatic, hydrodynamic and squeeze film bearing systems. Over the most recent couple of years, some researchers have explored peristaltic transport for the Rabinowitsch fluid model. Singh and Singh (2014) investigated peristaltic flow in a tube using Rabinowitsch fluid model. Akbar and Nadeem (2014) studied Rabinowitsch fluid model in peristalsis. Maraj and Nadeem (2015) studied

International Journal of Mathematical, Engineering and Management Sciences
Vol. 3, No. 4, 450–471, 2018
https://dx.doi.org/10.33889/IJMEMS.2018.3.4-033

peristaltic flow in a curved channel for Rabinowitsch fluid. In the present paper, heat transfer and peristaltic transport of Rabinowitsch fluid flowing through a channel have been investigated.

The present investigation is motivated because none of the investigators above have studied the effect of heat transfer on flow characteristics of peristaltic flow in a uniform channel with the Rabinowitsch fluid model. The present work is helpful to enhance the knowledge of physiological fluid of pseudoplastic nature.

2. Analysis

Consider the flow of a non-Newtonian fluid complying Rabinowitsch fluid model through a channel of uniform thickness. Sinusoidal wave proliferates on the wall of the channel and moving with speed c. Taking (X,Y) as a rectangular coordinate in a fixed frame, the geometry of peristaltic flow is shown in Fig. 1.

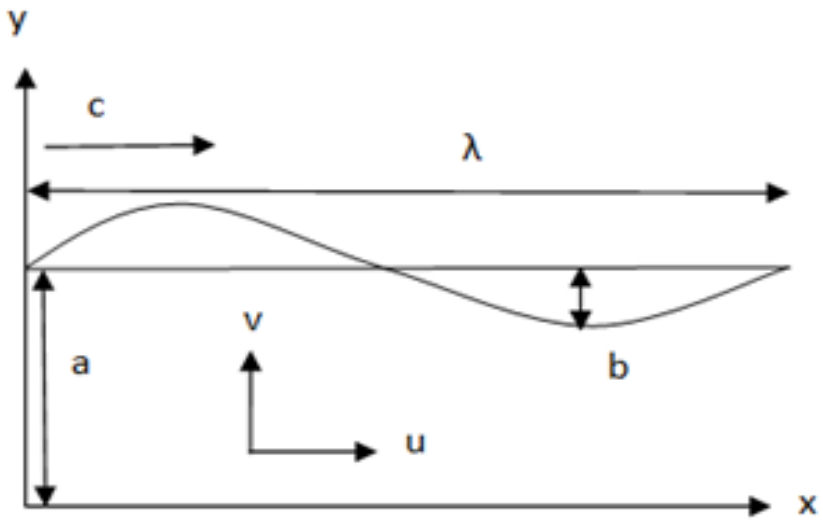

Fig. 1. Geometry of the peristaltic flow

The geometry of wall surface is given as

$$H(X,t') = a + b\,\mathrm{Sin}\left(\frac{2\pi(X - ct')}{\lambda}\right) \tag{2}$$

where a is half channel width, b is the amplitude of the wave, t' is time, λ is the wavelength.

Continuity equation

$$\frac{\partial U}{\partial X} + \frac{\partial V}{\partial Y} = 0 \tag{3}$$

International Journal of Mathematical, Engineering and Management Sciences
Vol. 3, No. 4, 450–471, 2018
https://dx.doi.org/10.33889/IJMEMS.2018.3.4-033

Momentum equation

$$\rho\left(\frac{\partial U}{\partial t'}+U\frac{\partial U}{\partial X}+V\frac{\partial U}{\partial Y}\right)=-\frac{\partial p}{\partial X}+\frac{\partial \tau_{XX}}{\partial X}+\frac{\partial \tau_{YX}}{\partial Y} \tag{4}$$

$$\rho\left(\frac{\partial V}{\partial t'}+U\frac{\partial V}{\partial X}+V\frac{\partial V}{\partial Y}\right)=-\frac{\partial p}{\partial Y}+\frac{\partial \tau_{XY}}{\partial X}+\frac{\partial \tau_{YY}}{\partial Y} \tag{5}$$

Energy equation

$$\rho c_p\left(\frac{\partial T}{\partial t'}+U\frac{\partial T}{\partial X}+V\frac{\partial T}{\partial Y}\right)=K\left(\frac{\partial^2 T}{\partial X^2}+\frac{\partial^2 T}{\partial Y^2}\right)+\tau_{XX}\frac{\partial U}{\partial X}+\tau_{YY}\frac{\partial V}{\partial Y}+\tau_{YX}\left(\frac{\partial U}{\partial Y}+\frac{\partial V}{\partial X}\right) \tag{6}$$

where U and V are components of velocity in X and Y directions respectively in a fixed frame of reference, c_p is specific heat at constant pressure, T is temperature, K is thermal conductivity, p is pressure, ρ is density, t' is time.

The transformation between fixed frame and wave frame is given by

$$u'=U-c, v'=V, x'=X-ct', y=Y \tag{7}$$

where u', v', x', y' are axial velocity, transverse velocity, axial coordinate and transverse coordinate respectively in wave frame.

Introducing non-dimensional parameters as follows

$$u=\frac{u'}{c}, v=\frac{v'}{c\delta}, x=\frac{x'}{\lambda}, y=\frac{y'}{a}, h=\frac{H}{a}, \delta=\frac{a}{\lambda}, p=\frac{p'a^2}{\mu c\lambda}, \mathrm{Re}=\frac{\rho a c}{\mu}, \theta=\frac{T-T_o}{T_o}, t=\frac{ct'}{\lambda},$$

$$\mathrm{Pr}=\frac{\mu c_p}{K}, Ec=\frac{c^2}{T_o c_p}, \phi=\frac{b}{a}, \tau_{xy}=\frac{a\tau'_{xy}}{c\mu}, \tau_{xx}=\frac{a\tau'_{xx}}{c\mu}, \tau_{yy}=\frac{a\tau'_{yy}}{c\mu}, \alpha=\frac{c^2\mu^2}{a}\gamma \tag{8}$$

Using Eq. (7) and Eq. (8) in Eq. (1), Eq. (2), Eq. (3), Eq. (4), Eq. (5) and Eq. (6) with the assumption of long wavelength and low Reynolds number approximation, we get

$$\tau_{yx}+\alpha\tau_{yx}^3=\frac{\partial u}{\partial y} \tag{9}$$

$$h=1+\phi\,\mathrm{Sin}(2\pi x) \tag{10}$$

International Journal of Mathematical, Engineering and Management Sciences
Vol. 3, No. 4, 450–471, 2018
https://dx.doi.org/10.33889/IJMEMS.2018.3.4-033

$$\frac{\partial \tau_{yx}}{\partial y} = \frac{\partial p}{\partial x} \tag{11}$$

$$\frac{\partial p}{\partial y} = 0 \tag{12}$$

$$\frac{\partial^2 \theta}{\partial y^2} = -Br\,\tau_{yx}\frac{\partial u}{\partial y} \tag{13}$$

where the dimensionless quantities α, ϕ, Ec and Br are the parameters of pseudoplasticity, amplitude ratio, Eckert number and Prandlt number respectively.

The boundary conditions for equations, Eq. (11-13) are as follow

$$\begin{cases} u = -1 \quad at \quad y = h \\ \dfrac{\partial u}{\partial y} = 0 \quad at \quad y = 0 \\ \dfrac{\partial \theta}{\partial y} = 0 \quad at \quad y = 0 \\ \theta = 0 \quad at \quad y = h \end{cases} \tag{14}$$

On solving Eq. (11) and Eq. (13) with boundary conditions Eq. (14), we get

$$u = \left(\frac{y^2 - h^2}{2}\right)\frac{dp}{dx} + \alpha\left(\frac{dp}{dx}\right)^3\left(\frac{y^4 - h^4}{4}\right) - 1 \tag{15}$$

$$\theta = Br\left(\frac{dp}{dx}\right)^2\left(\frac{\left(h^4 - y^4\right)}{12} + \alpha\frac{\left(h^6 - y^6\right)}{30}\left(\frac{dp}{dx}\right)^2\right) \tag{16}$$

where Brinkman Number $\left(Br\right) = Ec.\Pr$.

The coefficient of heat transfer $\left(\Omega\right)$ at the wall is given by

$$\Omega = -2\pi\phi\,\mathrm{Cos}\left(2\pi x\right)Br\left(\frac{dp}{dx}\right)^2\left(\frac{h^3}{3} + \alpha\left(\frac{dp}{dx}\right)^2\frac{h^5}{5}\right) \tag{17}$$

The corresponding stream function (cf. Appendix A) is obtained as:

$$\psi = \left(\frac{y^3}{6} - \frac{y\,h^2}{2}\right)\frac{dp}{dx} + \alpha\left(\frac{dp}{dx}\right)^3\left(\frac{y^5}{20} - \frac{y\,h^4}{4}\right) - y \tag{18}$$

International Journal of Mathematical, Engineering and Management Sciences
Vol. 3, No. 4, 450–471, 2018
https://dx.doi.org/10.33889/IJMEMS.2018.3.4-033

The volume flow rate in fixed frame (Q') and in wave frame (q') is given by

$$Q' = \int_0^H U\, dY \tag{19}$$

$$q' = \int_0^H u\, dy \tag{20}$$

Using Eq. (7), Eq. (19) and Eq. (20)

$$Q' = q' + cH \tag{21}$$

Average flow $\hat{Q} = \frac{1}{T}\int_0^T \bar{Q}\, dt$ over the time $T = \frac{\lambda}{c}$, we have

$$\hat{Q} = q' + ca \tag{22}$$

This can be reduced in dimensionless form as

$$Q = q + 1 \tag{23}$$

where $q = \frac{q'}{ac} = \int_0^h u dy;\quad Q = \frac{\hat{Q}}{ac}$ (24)

Using Eq. (15) in Eq. (24),

$$\frac{dp}{dx} + \frac{3}{5}\alpha h^2 \left(\frac{dp}{dx}\right)^3 + 3\left(\frac{q+h}{h^3}\right) = 0 \tag{25}$$

In the limiting case, as $\alpha \to 0$ Eq. (25) reduces to result of Shapiro et al. (1969)

$$\frac{dp}{dx} = -3\left(\frac{q+h}{h^3}\right) \tag{26}$$

As Eq. (25) is the nonlinear equation of first order, it is difficult to find an analytic solution of pressure, however, for small values of the pseudoplasticity parameter $(\alpha << 1)$, Eq. (25) can be perturbed as follows

$$p = p_o + \alpha\, p_1 \tag{27}$$

so that

International Journal of Mathematical, Engineering and Management Sciences
Vol. 3, No. 4, 450–471, 2018
https://dx.doi.org/10.33889/IJMEMS.2018.3.4-033

$$\frac{dp}{dx} = -3\left(\frac{q+h}{h^3}\right) + \frac{81}{5}\alpha\frac{(q+h)^3}{h^7} \tag{28}$$

Using Eq. (23) in Eq. (28)

$$\frac{dp}{dx} = -3\left(\frac{Q-1+h}{h^3}\right) + \frac{81}{5}\alpha\frac{(Q-1+h)^3}{h^7} \tag{29}$$

The pressure rise and friction force are given by

$$\Delta p = \int_0^1 \frac{dp}{dx}\,dx \tag{30}$$

$$F = \int_0^1 h\left(-\frac{dp}{dx}\right)dx \tag{31}$$

3. Results and Discussion

In the present section of this paper, the attempts have been made to analyze the effects of various parameters on pressure gradient, fluid velocity, pressure rise, friction force and fluid temperature in case of Newtonian, dilatant and pseudoplastic fluids. Looking at the need to scrutinize the qualitative effects of different parameters, the graphs have been drawn using MATHEMATICA. In order to perform numerical computation, following values of the parameters have been used:
Amplitude ratio: $0 < \phi < 1$.

The parameter of pseudoplasticity: $-0.1 < \alpha < 0.1$.

The variation of pressure rise against the flow rate is shown in Fig. 2 for the parameter of pseudoplasticity $\alpha = -0.1, 0, 0.1$ and amplitude ratio $\phi = 0.3, 0.4$. The pressure rise linearly connected to flow rate for the case of Newtonian fluids which agrees with the result derived by Shapiro et al. (1969) whereas the same is non-linear in the pseudoplastic and dilatant fluid. It is unambiguous from Fig. 2 that when the parameter of pseudopalsticity is large then the fluid will be thinner and small pressure rise is observed as compared to Newtonian and dilatant fluids in peristaltic pumping domain. The pressure rise for Newtonian fluid increases by increasing amplitude ratio in the region of peristaltic pumping whereas shows opposite behavior in the co-pumping region. The result of pressure rise for Newtonian fluid at agrees with the established result of Vajravelu et al. (2005) for yield stress 0 and flow behavior index 1. Pressure rise decreases more rapidly for dilatant nature of the fluid in the peristaltic pumping region. Maximum pressure rise is observed for dilatant fluid at zero flow rate.

International Journal of Mathematical, Engineering and Management Sciences
Vol. 3, No. 4, 450–471, 2018
https://dx.doi.org/10.33889/IJMEMS.2018.3.4-033

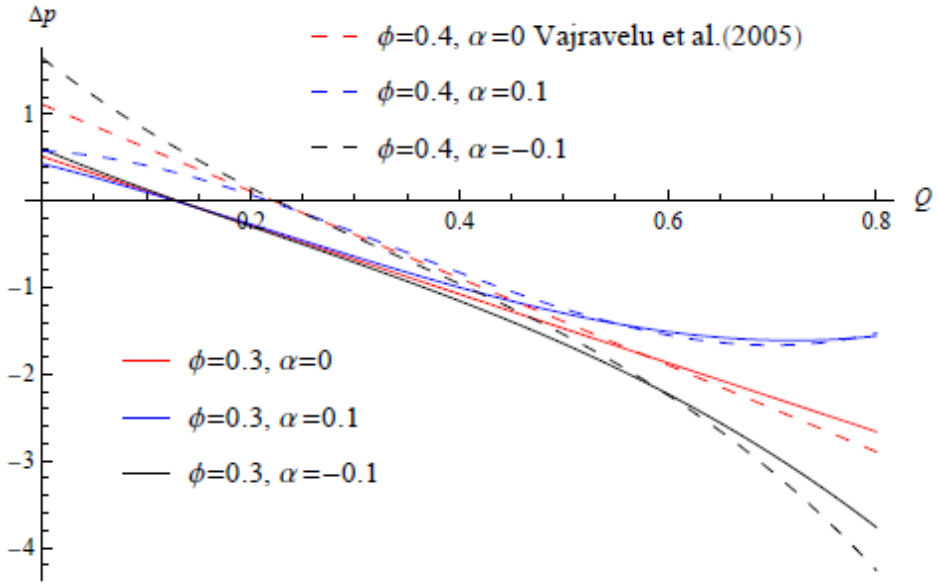

Fig. 2. Pressure rise vs. averaged flow rate for various values of ϕ, α

Fig. 3 shows the variation of friction force against the flow rate for the parameter of pseudoplasticity $\alpha = -0.1, 0, 0.1$ and amplitude ratio $\phi = 0.3, 0.4$. It is apparent that the impact of amplitude ratio on friction force is in contrast to the effect of amplitude ratio on pressure rise for Newtonian fluid. The result of friction force for Newtonian fluid at $\phi = 0.4$ is consistent with the established result of Vajravelu et al. (2005) for yield stress 0 and flow behavior index 1. The similar behavior is observed for pseudoplastic and dilatant fluids.

Fig. 4 represents the change in pressure rise against the amplitude ratio for the parameter of pseudoplasticity $\alpha = -0.1, 0, 0.1$ and flow rate $Q = 0.3, 0.4$. Fig. 4 explains that pressure rise increases indefinitely for Newtonian and dilatant nature of the fluid at a constant flow rate but for pseudoplastic fluid, firstly pressure rise increases and then decreases indefinitely. On increasing flow rate pressure rise decreases at zero amplitude ratio (at no pumping).

International Journal of Mathematical, Engineering and Management Sciences
Vol. 3, No. 4, 450–471, 2018
https://dx.doi.org/10.33889/IJMEMS.2018.3.4-033

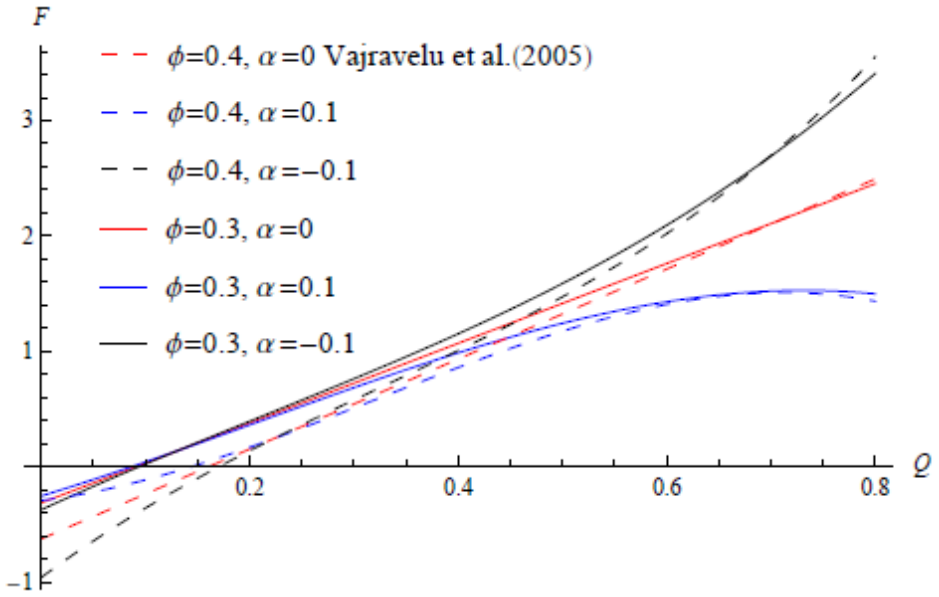

Fig. 3. Friction force vs. averaged flow rate for various values of ϕ, α

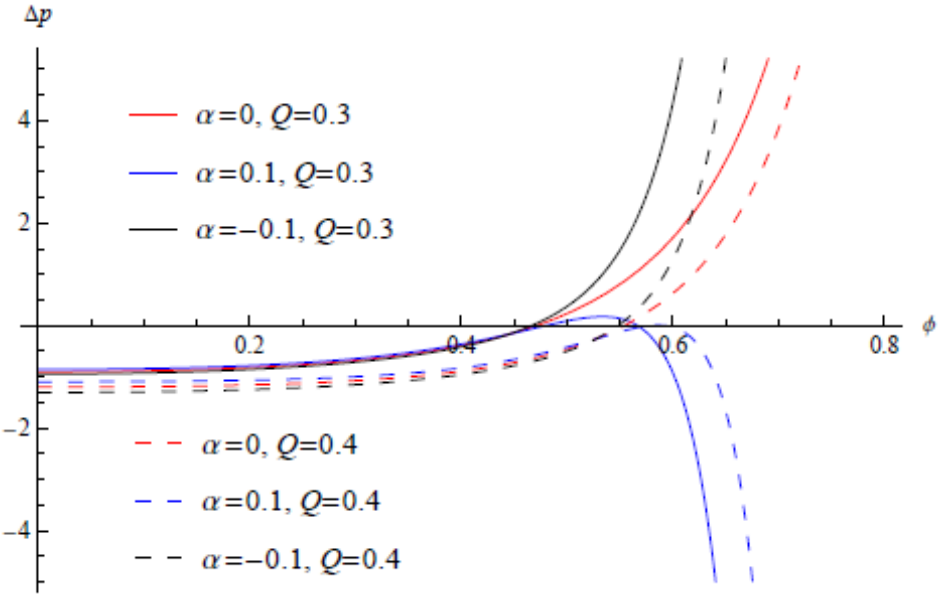

Fig. 4. Pressure rise vs. amplitude ratio for various values of Q, α

International Journal of Mathematical, Engineering and Management Sciences
Vol. 3, No. 4, 450–471, 2018
https://dx.doi.org/10.33889/IJMEMS.2018.3.4-033

Fig. 5 gives the information about the change in friction force against the amplitude ratio for the parameter of pseudoplasticity $\alpha = -0.1, 0, 0.1$ and flow rate $Q = 0.3, 0.4$. It is apparent that the effect of flow rate on friction force is in contrast to the effect of flow rate on pressure rise.

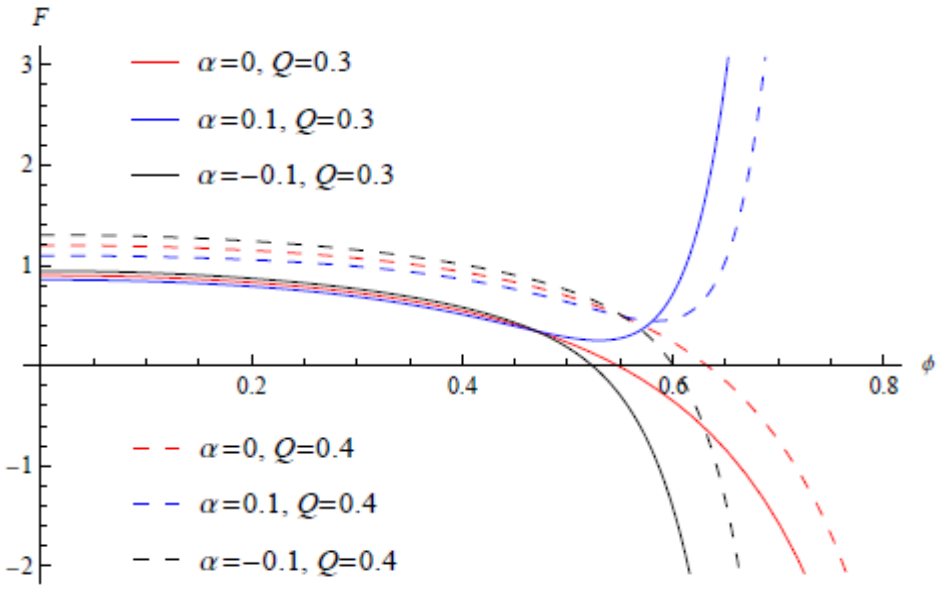

Fig. 5. Friction force vs. amplitude ratio for various values of Q, α

Fig. 6(a-b) explain the behavior of pressure gradient with change in the rate of flow and amplitude ratio. Pressure gradient starts decreasing when the flow rate starts rising. The small pressure gradient is observed for $x \in [0, 0.6]$ and higher pressure gradient occurs for $x \in [0.6, 0.9]$. The maximum pressure gradient is observed for dilatant nature of the fluid and minimum pressure gradient is observed for pseudoplastic fluid when $x \in [0, 0.6]$. Pressure gradient increases with increases in amplitude ratio for $x \in [0.6, 0.9]$. Unnoticeable change in pressure gradient is observed for $x \in [0, 0.5]$ with the change in amplitude ratio. The maximum pressure gradient is observed for dilatant nature of the fluid and minimum pressure gradient is observed for pseudoplastic fluid when $x \in [0.6, 0.9]$.

Variation of velocity for various values of flow rate and amplitude ratio has been presented in Fig. 7(a-b). For Newtonian fluid, the magnitude of velocity is noticed to be highest in the middle of the channel. The magnitude of velocity decreases for pseudoplastic fluid and increases for dilatant nature of the fluid with an increase in flow rate. Opposite behavior is seen at the wall of the channel. A similar behavior is observed with an increasing value in amplitude ratio.

International Journal of Mathematical, Engineering and Management Sciences
Vol. 3, No. 4, 450–471, 2018
https://dx.doi.org/10.33889/IJMEMS.2018.3.4-033

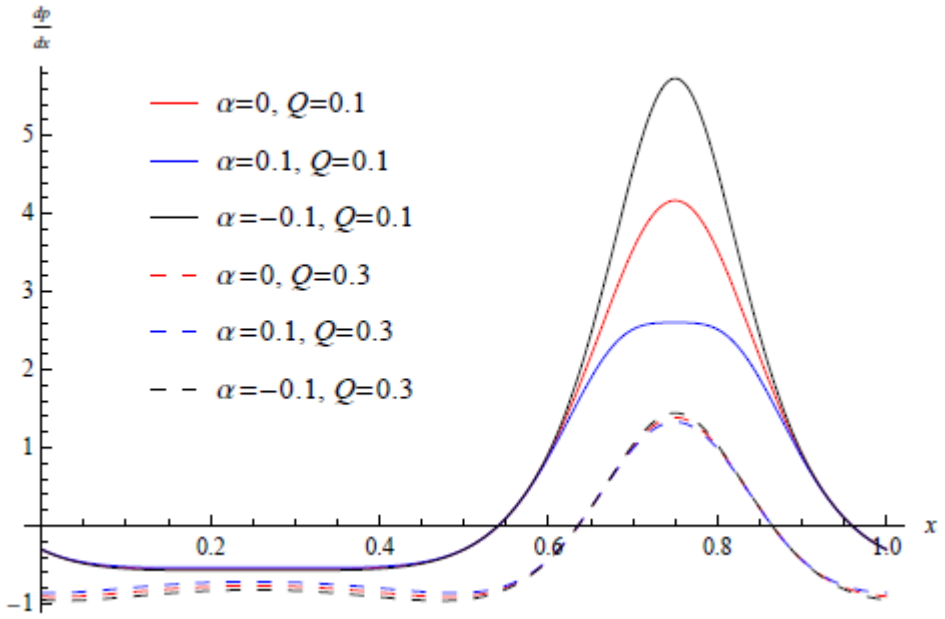

Fig. 6 (a). Pressure gradient for various values of Q, α at $\phi = 0.4$

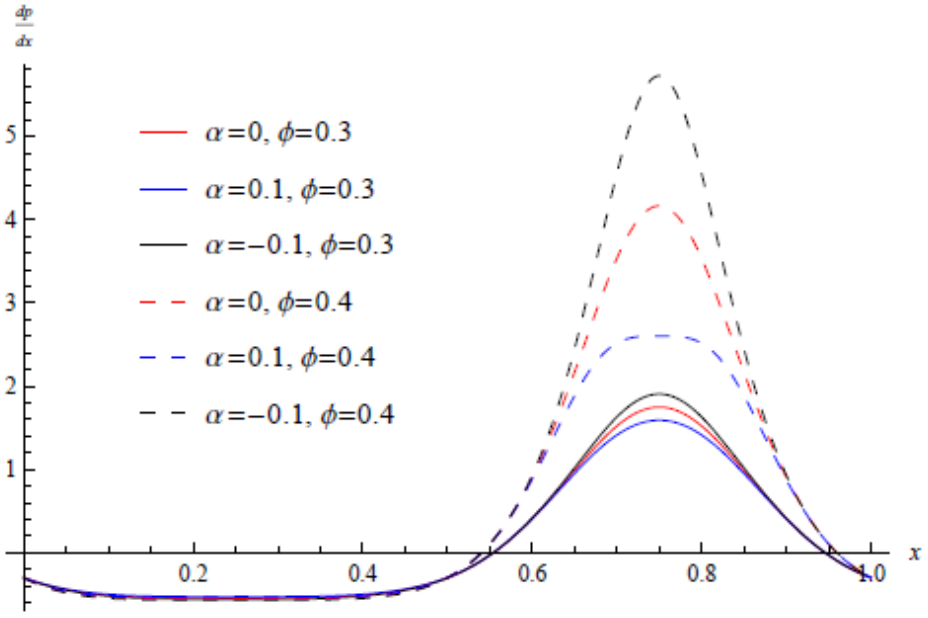

Fig. 6 (b). Pressure gradient for various values of ϕ, α at $Q = 0.1$

International Journal of Mathematical, Engineering and Management Sciences
Vol. 3, No. 4, 450–471, 2018
https://dx.doi.org/10.33889/IJMEMS.2018.3.4-033

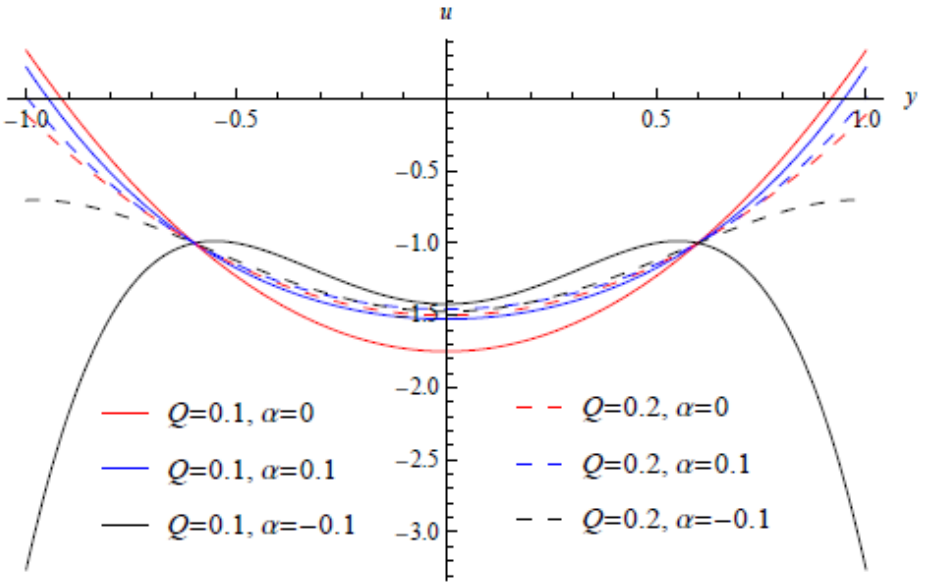

Fig. 7 (a). Velocity profile for different value of Q, α at $\phi = 0.4, x = 0.75$

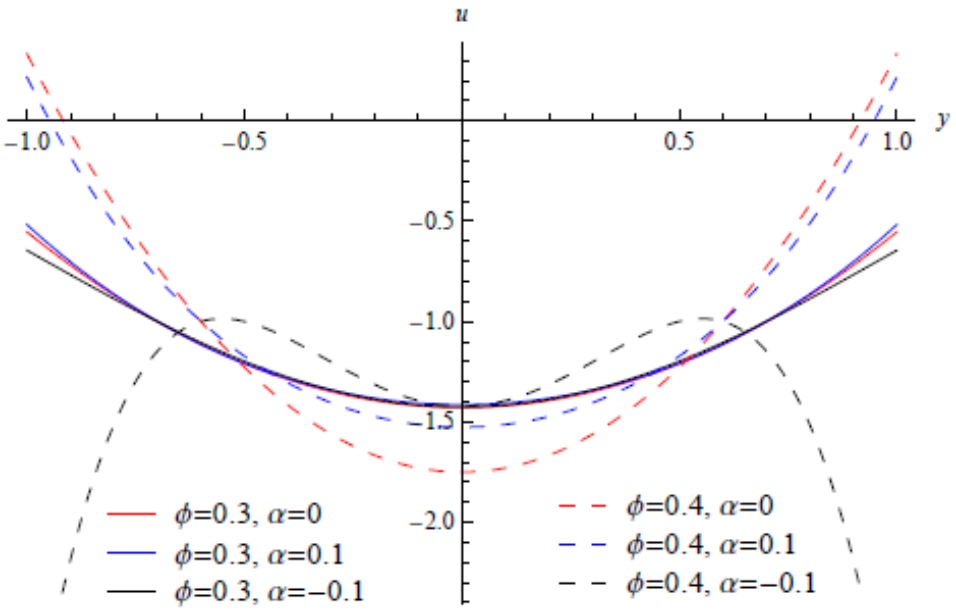

Fig. 7 (b). Velocity profile for different value of ϕ, α at $Q = 0.1, x = 0.75$

International Journal of Mathematical, Engineering and Management Sciences
Vol. 3, No. 4, 450–471, 2018
https://dx.doi.org/10.33889/IJMEMS.2018.3.4-033

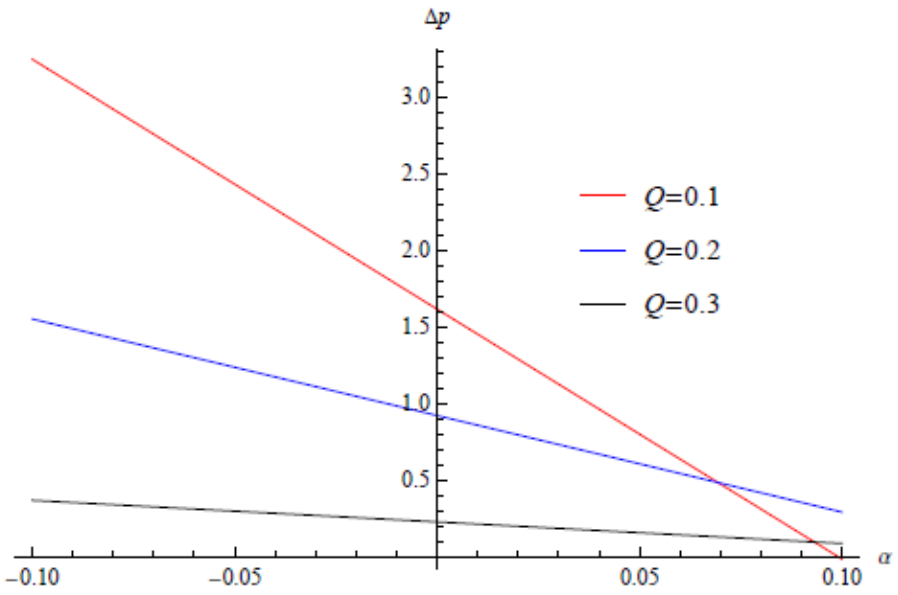

Fig. 8. Pressure rise vs. parameter of pseudoplasticity for various values of Q at $\phi = 0.5$

Fig. 8 depicts the change in pressure rise against the parameter of pseudoplasticity at flow rates $Q = 0.1,\ 0.2,\ 0.3$. One can notice that while moving from Newtonian to pseudoplastic fluid the pressure rise decreases, whereas while moving from Newtonian to dilatant fluid, the pressure rise increases irrespective of the value of flow rate.

The variation of temperature with y at $x = 0$ and at $x = 0.2$ of the channel is shown in Fig. 9 for $\alpha = -0.1, 0, 0.1$, $Br = 0.2$, $Q = 0.3$, $\phi = 0.4$. The increment in the temperature is analyzed by moving from the inlet $(x = 0)$ toward downstream $(x = 0.2)$. It is also clear that there is minor change noticed in the temperature close to the middle of the channel but a fast change in temperature is observed in the vicinity the wall of the channel. Maximum temperature is obtained for dilatant fluid and minimum temperature is obtained for pseudoplastic fluid at the middle of the channel.

Fig. 10 depicts the variation of temperature against y for $\alpha = -0.1, 0, 0.1$, $Br = 0.2, 0.3$, $Q = 0.3$, $\phi = 0.4$, $x = 0.2$. It is observed that with an increase in Brinkman number, temperature increases in the middle of the channel. Minimum temperature is obtained for pseudoplastic fluid (thinner fluid) whereas maximum temperature is observed for dilatant nature of the fluid for a given value of the Brinkman number in the middle of the channel.

International Journal of Mathematical, Engineering and Management Sciences
Vol. 3, No. 4, 450–471, 2018
https://dx.doi.org/10.33889/IJMEMS.2018.3.4-033

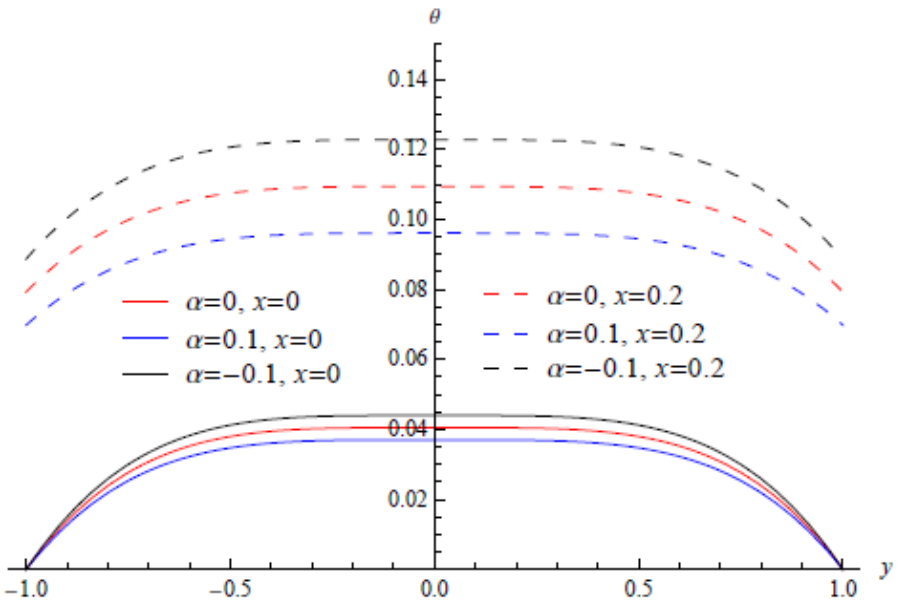

Fig. 9. Effect of α on temperature at $\phi = 0.4, Br = 0.2, Q = 0.3$ at inlet $(x = 0)$ as well as downstream $(x = 0.2)$

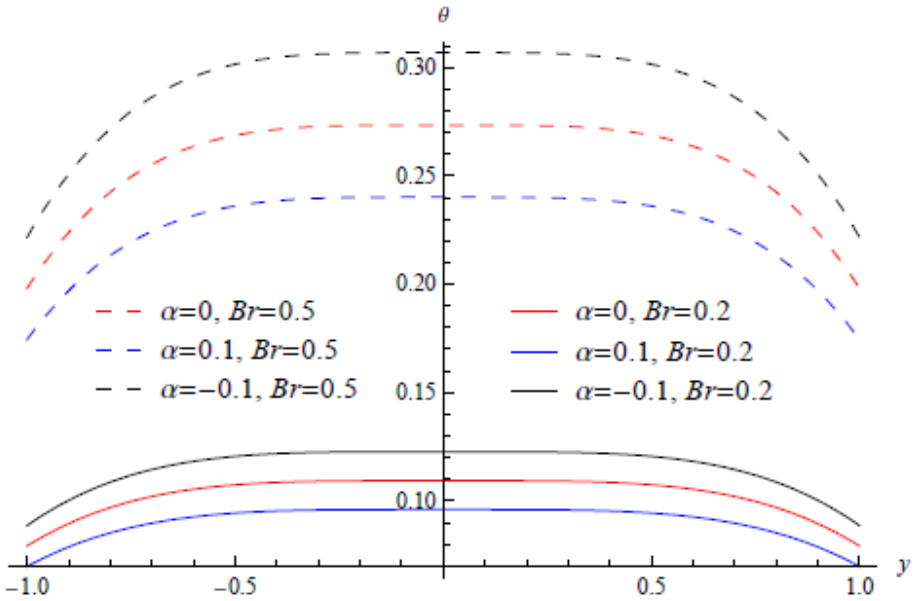

Fig. 10. Effect of Br, α on temperature at $\phi = 0.4,\ Q = 0.3,\ x = 0.2$

International Journal of Mathematical, Engineering and Management Sciences
Vol. 3, No. 4, 450–471, 2018
https://dx.doi.org/10.33889/IJMEMS.2018.3.4-033

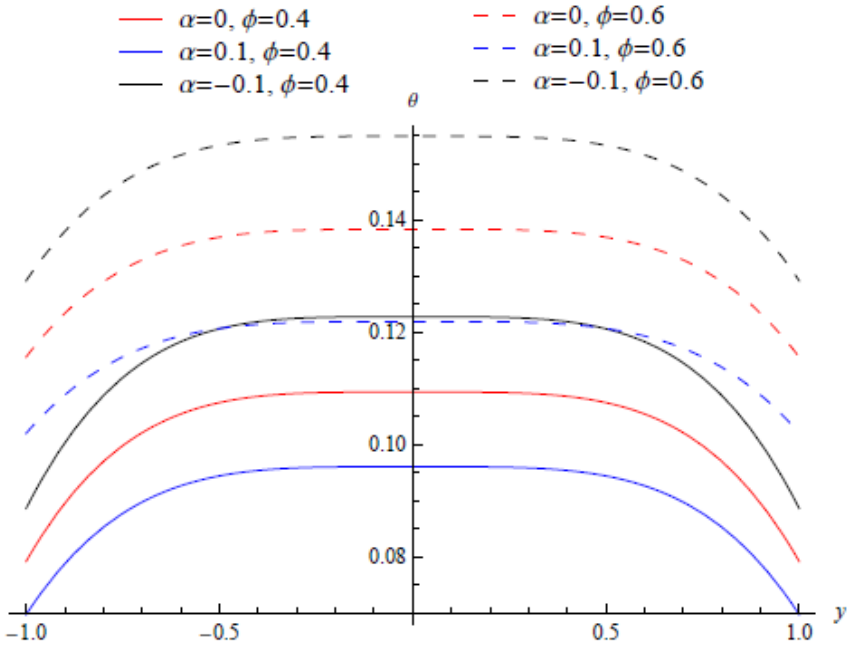

Fig. 11. Effect of ϕ, α on temperature at $Br = 0.2,\ Q = 0.3,\ x = 0.2$

Fig. 11 shows change in temperature against y for $\alpha = -0.1, 0, 0.1$, $Br = 0.2$, $Q = 0.3$, $\phi = 0.4, 0.6$, $x = 0.2$. It is evident from Fig. 11 that temperature increases with increase in amplitude ratio. Maximum temperature is obtained in the middle of the channel and decreases near the wall of the channel for all types of fluid.

The temperature profile is plotted against y as illustrated in Fig. 12 for $\alpha = -0.1, 0, 0.1$, $Br = 0.2$, $Q = 0.3, 0.4$, $\phi = 0.4$, $x = 0.2$. It is clear from Fig. 12 that temperature decreases continuously by an increase in flow rate for pseudeoplastic, dilatant and Newtonian fluid.

Fig. 13(a-b) shows the variation of heat transfer coefficient along the axial direction for different value of $Q = 0.1, \alpha = 0, 0.1, -0.1, Br = 0.2$ (a) $\phi = 0.3$ (b) $\phi = 0.4$. It is clear from Fig. 13(a-b) that the magnitude of the heat transfer coefficient i*n*creases with increase in amplitude ratio irrespective of the fluids nature. The maximum and minimum magnitude of the heat transfer coefficient is observed for dilatant and pseudeoplastic fluid respectively. This analysis is expected to be useful in physiology as well as in industry.

International Journal of Mathematical, Engineering and Management Sciences
Vol. 3, No. 4, 450–471, 2018
https://dx.doi.org/10.33889/IJMEMS.2018.3.4-033

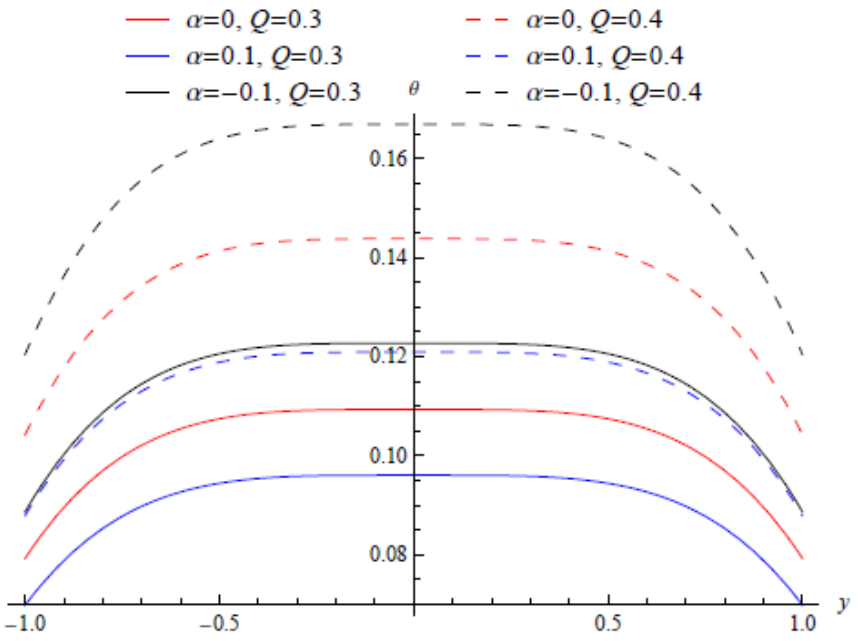

Fig. 12. Effect of Q, α on temperature at $Br = 0.2,\ \phi = 0.4,\ x = 0.2$

(a)

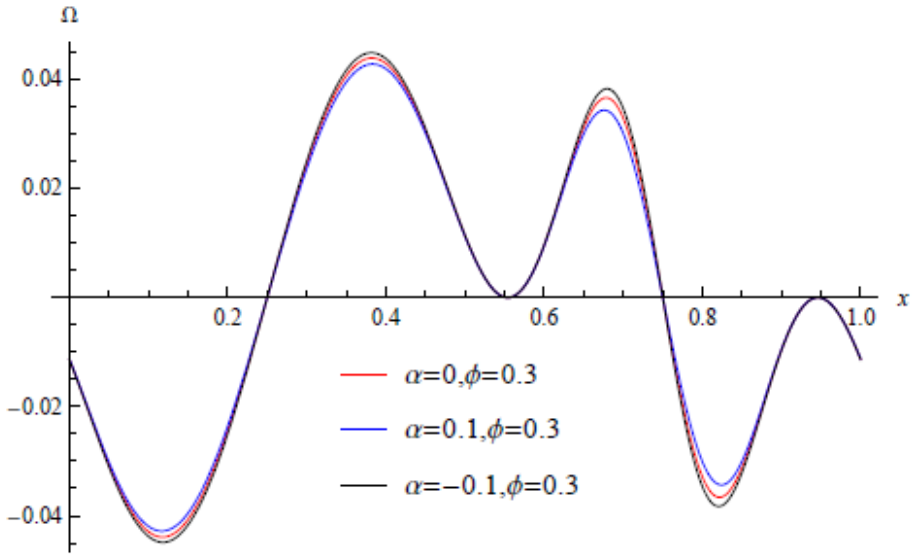

International Journal of Mathematical, Engineering and Management Sciences
Vol. 3, No. 4, 450–471, 2018
https://dx.doi.org/10.33889/IJMEMS.2018.3.4-033

(b)

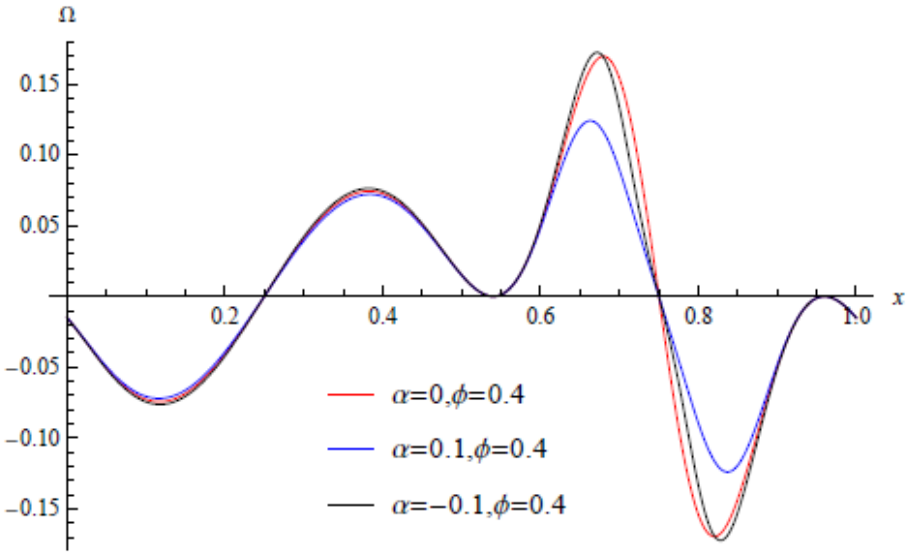

Fig. 13. Heat transfer coefficient $\alpha = 0, 0.1, -0.1, Br = 0.2, Q = 0.1$ at (a) $\phi = 0.3$ (b) $\phi = 0.4$

(a)

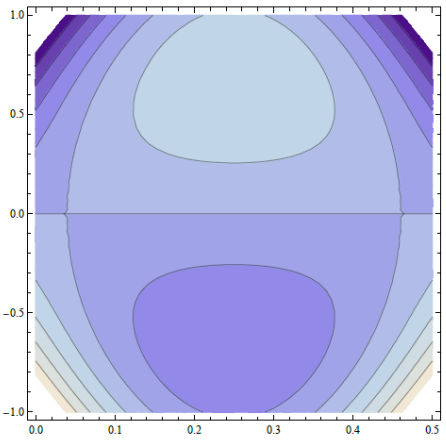

International Journal of Mathematical, Engineering and Management Sciences
Vol. 3, No. 4, 450–471, 2018
https://dx.doi.org/10.33889/IJMEMS.2018.3.4-033

(b)

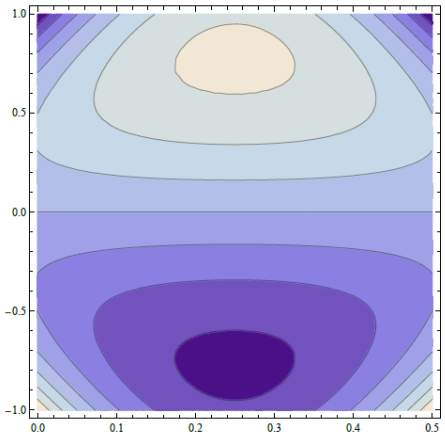

(c)

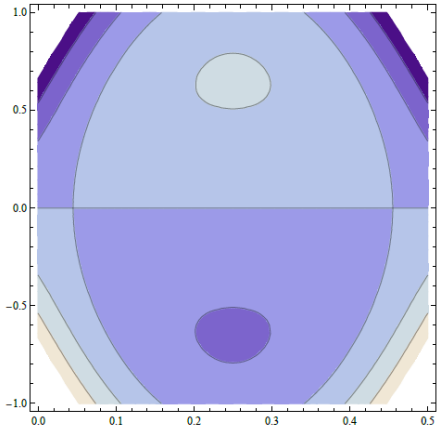

Fig. 14. Stream lines when $Q = 0.8, \phi = 0.6$ (a) $\alpha = 0.1$ (b) $\alpha = 0$ (c) $\alpha = -0.1$

Fig. 14(a-c) shows the effect of coefficient of pseudoplasticity on the formation of bolus for $Q = 0.8$, $\phi = 0.6$. It is clear that the size of bolus decreases when nature of the fluid changes gradually from pseudoplastic (thinner fluid) to dilatant. More number of the boluses is formed for Newtonian fluid as compared to pseudoplastic and dilatant fluid. Fig. 15(a-b) reveals the interesting fact that with an increase in amplitude ratio, the size of the bolus decreases and gets shifted towards the wall of the channel.

International Journal of Mathematical, Engineering and Management Sciences
Vol. 3, No. 4, 450–471, 2018
https://dx.doi.org/10.33889/IJMEMS.2018.3.4-033

(a)

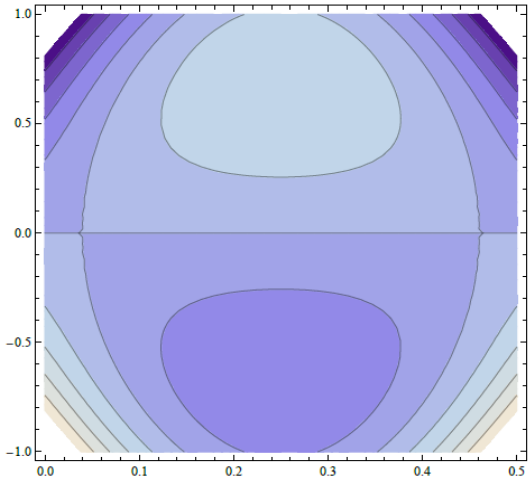

(b)

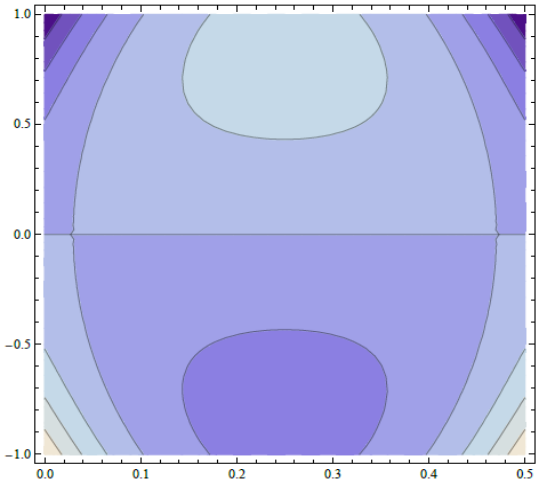

Fig. 15. Stream lines when $Q = 0.8, \alpha = 0.1$ (a) $\phi = 0.6$ (b) $\phi = 0.8$

4. Conclusions

The following conclusion can be summarized:

- Pressure rise for pseudopalstic fluid is small as compared to Newtonian and dilatant fluid in the peristaltic pumping region.
- Friction force reflects the reverse trend to that of pressure rise.

- It is noticed that as the nature of fluid changes from Newtonian to pseudoplastic, the pressure rise decreases, whereas while changing from Newtonian to dilatant nature, the pressure rise increases irrespective of the value of flow rate.
- It is clearly seen that the magnitude of velocity is maximum for Newtonian fluid at the middle of the channel and decreases with pseudoplasticity but increases with dilatant nature of the fluid.
- It is analyzed that on moving from the inlet $(x=0)$ to downstream $(x=0)$, temperature decreases for all types of fluid.
- With increasing amplitude ratio, temperature increases for all types of fluid.
- It is seen that bolus size decreases when nature of the fluid shifted from pseudoplastic (thinner fluid) to dilatant. More number of the boluses is formed for Newtonian fluid as compared to pseudoplastic and dilatant fluid.
- The consequence of increasing amplitude ratio comes in the form of decrease in the size of the trapped bolus.

References

Akbar, N. S., & Butt, A. W. (2015). Heat transfer analysis for the peristaltic flow of Herschel–Bulkley fluid in a nonuniform inclined channel. *Zeitschrift für Naturforschung A-A Journal of Physical Sciences, 70*(1), 23-32.

Akbar, N. S., & Nadeem, S. (2014). Application of rabinowitsch fluid model in peristalsis. *Zeitschrift für Naturforschung A-A Journal of Physical Sciences, 69*(8-9), 473-480.

Bhatt, S. S., Medhavi, A., Gupta, R. S., & Singh, U. P. (2017). Effects of heat transfer during peristaltic transport in nonuniform channel with permeable walls. *Journal of Heat Transfer, 139*(014502), 1-6.

Chaube, M. K., Tripathi, D., Beg, O. A., Sharma, S., & Pandey, V. S. (2015). Peristaltic creeping flow of power law physiological fluids through a nonuniform channel with slip effect. *Applied Bionics and Biomechanics*, 1-10.

Fung, Y. C., & Yih, C. S. (1968). Peristaltic transport. *Journal of Applied Mechanics, 35*(4), 669-675.

Gupta, B. B., & Seshadri, V. (1976). Peristaltic pumping in non-uniform tubes. *Journal of Biomechanics, 9*(2), 105-109.

Kaimal, M. R. (1978). Peristaltic pumping of a newtonian fluid with particles suspended in it at low reynolds number under long wavelength approximations. *Journal of Applied Mechanics, 45*(1), 32-36.

Latham, T. W. (1966). Fluid motion in a peristaltic pump. *M.S. Thesis, M. I. T. Massachusetts Institute of Technology, Cambridge*, 1-74.

Machireddy, G. R., & Kattamreddy, V. R. (2016). Impact of velocity slip and joule heating on MHD peristaltic flow through a porous medium with chemical reaction. *Journal of the Nigerian Mathematical Society, 35*(1), 227-244.

Maraj, E. N., & Nadeem, S. (2015). Application of rabinowitsch fluid model for the mathematical analysis of peristaltic flow in a curved channel. *Zeitschrift für Naturforschung A-A Journal of Physical Sciences, 70*(7), 513-520.

Misra, J. C., & Pandey, S. K. (2002). Peristaltic transport of blood in small vessels: study of a mathematical model. *Computers and Mathematics with Applications, 43*(8-9), 1183-1193.

Pandey, S. K., & Chaube, M. K. (2011). Study of wall properties on peristaltic transport of a couple stress fluid. *Meccanica*, *46*(6), 1319-1330.

Radhakrishnamacharya, G., & Murty, V. R. (1993). Heat transfer to peristaltic transport in a non-uniform channel. *Defence Science Journal*, *43*(3), 275-280.

Raju, K. K., & Devanathan, R. (1972). Peristaltic motion of a non-Newtonian fluid. *Rheologica Acta*, *11*(2), 170-178.

Reddy, R. H., Kavitha, A., Sreenadh, S., & Saravana, R. (2011). Effect of induced magnetic field on peristaltic transport of a carreau fluid in an inclined channel filled with porous material. *International Journal of Mechanical and Materials Engineering*, *6*(2), 240-249.

Saravana, R., Reddy, R. H., Goud, J. S., & Sreenadh, S. (2016). MHD peristaltic flow of a hyperbolic tangent fluid in a non-uniform channel with heat and mass transfer. *IOP Conference Series: Materials Science and Engineering*, *263*, 1-15, *Article ID:062006*.

Shapiro, A. H., Jaffrin, M. Y., & Weinberg, S. L. (1969). Peristaltic pumping with long wavelengths at low reynolds number. *Journal of Fluid Mechanics*, *37*(4), 799-825.

Singh, B. K., & Singh, U. P. (2014). Analysis of peristaltic flow in a tube: Rabinowitsch fluid model. *International Journal of Fluids Engineering*, *6*(1), 1-8.

Singh, U. P. (2013). Application of rabinowitsch fluid model to pivoted curved slider bearings. *Archive of Mechanical Engineering*, *60*(2), 247-267.

Singh, U. P., Gupta, R. S., & Kapur, V. K. (2011). On the steady performance of hydrostatic thrust bearing: Rabinowitsch fluid model. *Tribology Transactions, 54*(5), 723-729.

Singh, U. P., Gupta, R. S., & Kapur, V. K. (2012). On the steady performance of annular hydrostatic thrust bearing: Rabinowitsch fluid model. *ASME Journal of Tribology*, *134*, 1-5, *Article ID:* 044502.

Singh, U. P., Gupta, R. S., & Kapur, V. K. (2013). On the squeeze film characteristics between a long cylinder and a flat plate: Rabinowitsch model. *Proceedings of the Institution of Mechanical Engineers, Part J: Journal of Engineering Tribology, 227*(1), 34-42.

Singh, U., Gupta, R., & Kapur, V. (2011). Effects of inertia in the steady state pressurised flow of a non-Newtonian fluid between two curvilinear surfaces of revolution: Rabinowitsch fluid model. *Chemical and Process Engineering, 32(*4), 333-349.

Sinha, A., Shit, G. C., & Ranjit, N. K. (2015). Peristaltic transport of MHD flow and heat transfer in an asymmetric channel: Effects of variable viscosity, velocity-slip and temperature jump. *Alexandria Engineering Journal*, *54*(3), 691-704.

Srinivas, S., & Kothandapani, M. (2008). Peristaltic transport in an asymmetric channel with heat transfer a note. *International Communications in Heat and Mass Transfer*, *35*(4), 514-522.

Vajravelu, K., Sreenadh, S., & Babu, V. R. (2005). Peristaltic pumping of a Herschel–Bulkley fluid in a channel. *Applied Mathematics and Computation*, *169*(1), 726-735.

Wada, S., & Hayashi, H. (1971). Hydrodynamic lubrication of journal bearings by pseudo-plastic lubricants: Part 2, experimental studies. *Bulletin of the Japan Society of Mechanical Engineers*, *14*(69), 279-286.

Yin, F., & Fung, Y. C. (1969). Peristaltic waves in circular cylindrical tubes. *Journal of Applied Mechanics, 36*(3), 579-587.

International Journal of Mathematical, Engineering and Management Sciences
Vol. 3, No. 4, 450–471, 2018
https://dx.doi.org/10.33889/IJMEMS.2018.3.4-033

Appendix (A)

Since $u = \frac{\partial \psi}{\partial y}$, integrating equation (15) and using the condition $\psi = 0$ at $y = 0$ we get

$$\psi = \left(\frac{y^3}{6} - \frac{yh^2}{2} \right) \frac{dp}{dx} + \alpha \left(\frac{dp}{dx} \right)^3 \left(\frac{y^5}{20} - \frac{yh^4}{4} \right) - y$$